
Revolutionizing Large Language Model Training through Dynamic Parameter Adjustment

Kaiye Zhou Shucheng Wang

China Mobile (Suzhou) Software Technology Co. Ltd.

Suzhou 215000, China

{zhoukaiye, wangshucheng}@cmss.chinamobile.com

Abstract: In the era of large language models, the demand for efficient use of computational resources has become critically important. Although parameter-efficient fine-tuning techniques have achieved results comparable to full fine-tuning, their application during the pre-training phase poses significant challenges. Specifically, employing parameter-efficient strategies at the onset of pre-training can severely compromise efficiency, especially in larger models. In this paper, building upon the fine-tuning method LoRA, we introduce a novel parameter-efficient training technique that frequently alters trainable part of parameters, facilitating effective pre-training. Our method not only achieves memory reductions and computational overhead comparable to current state-of-the-art parameter-efficient algorithms during the pre-training phase but also maintains accuracy levels comparable to those of full pre-training. We provide both theoretical analyses and empirical evidence to demonstrate the effectiveness of our approach.

1 Introduction

In recent years, the size of large language models (LLMs) has increased rapidly, a trend ignited by the advent of the transformer architecture [33]. To support the training of increasingly large models, various distributed training techniques have been employed. These include data parallelism [4, 19], the Zero Redundancy Optimizer [27] to optimize data splitting, tensor parallelism [28], and pipeline parallelism [16, 26] to partition the model itself. Despite these advancements, hardware resources are increasingly becoming a bottleneck as model sizes continue to expand [26]. For models exceeding one trillion parameters, the predominant approach is 3D parallelism, which integrates data, tensor, and pipeline parallelism. Presently, a significant portion of the inter-node communication overhead is attributed to data parallelism, required by the frequent communication of large quantities of parameter gradients.

To address these challenges, various parameter-efficient strategies have been proposed. Techniques such as model sparsification [1, 29] and progressive model pruning during training [7] have shown promise. Additionally, methods leveraging Singular Value Decomposition (SVD) to approximate full-rank matrices in low-rank spaces have been explored [30, 34, 38, 39].

Beyond the entire training process, several techniques focus on the fine-tuning phase to enhance adaptability and efficiency. For instance, the Adapter method [14, 13] introduces additional trainable layers while freezing the remaining parameters. Similarly, prefix-tuning [20] employs a small set of trainable vectors (prefixes) at the beginning of each transformer layer to enable adaptation to new tasks without altering the core pre-trained model parameters.

Another noteworthy fine-tuning strategy is Low-Rank Adaptation (LoRA) [15], which has attracted attention for its effectiveness and the fact that it introduces no additional computational overhead during inference. However, it is important to note that while these parameter-efficient methods like LoRA are highly effective for fine-tuning, directly applying them during the pre-training phase can lead to a considerable loss in model accuracy as observed in many prior works [34, 35, 24]. We hypothesize that this loss of accuracy is due to the premature use of low-rank training, which may cause the model to become trapped in a local minimum. In response, we aim to develop a strategy

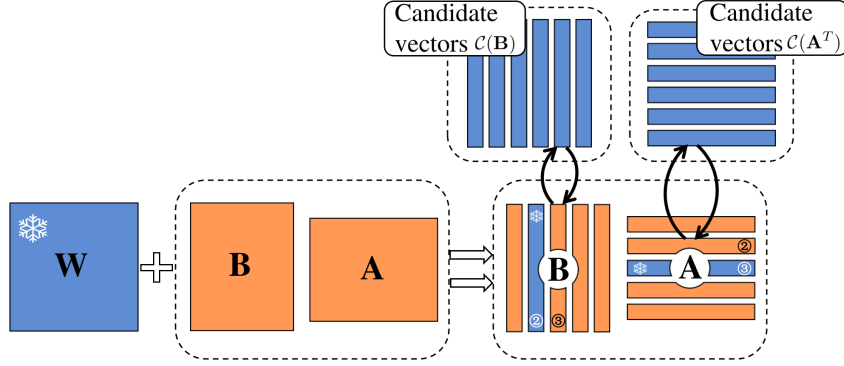


Figure 1: SwiLoRA: An enhanced LoRA with dynamic vector switching for pre-training. In traditional LoRA, an adapter \mathbf{BA} is added to the matrix \mathbf{W} of linear layers. \mathbf{B} and \mathbf{A} are trained while \mathbf{W} is kept frozen (as depicted in left part of the figure). SwiLoRA enhances this by dynamically switching vectors within \mathbf{B} and \mathbf{A} . The figure illustrates an example of this process: when the third column (labeled as black ③) of \mathbf{B} is switched, the corresponding third row (labeled as white ③) of \mathbf{A} is temporarily frozen. Similarly, when the second row (labeled as black ②) of \mathbf{A} is switched, the corresponding second column (labeled as white ②) of \mathbf{B} is also temporarily frozen.

that utilizes parameter-efficient training while frequently changing the trainable part of parameters. This approach is designed to mimic the behavior of full-rank training, potentially overcoming the limitations observed with early implementations of low-rank adaptations.

Our contribution:

- We have developed a novel strategy utilizing Low-Rank Adaptation (LoRA), termed SwiLoRA, which enables smooth adjustments to the trainable parameters of the LoRA matrices, as illustrated in Figure 1. This approach extends the application of LoRA to the pre-training stage with minimal loss of accuracy. Additionally, SwiLoRA is scalable to any model size, as it introduces negligible additional computational overhead.
- We propose a method for calculating optimal initial parameters for LoRA matrices and their associated candidate vectors introduced in our algorithm. This initiative is designed to accelerate the warm-up phase of training and ensure balanced updates of the LoRA matrices, thereby improving the overall efficiency of the training process.
- We conduct a theoretical analysis of the properties of the local linear system incorporating SwiLoRA, providing insights into how SwiLoRA affect the system’s dynamics and performance.

2 Methodology

A substantial body of research, such as various pruning methods [10, 3], has demonstrated that neural networks tend to exhibit low-rank characteristics after certain stages of training. Techniques for parameter-efficient fine-tuning, such as LoRA, capitalize on this observation. Concurrently, studies like [23, 9] have revealed that overparameterization in neural networks can lead to implicit regularization, thereby enhancing generalization. These findings underscore the importance of training with full parameters during the initial phase. Further empirical evidence supporting this phenomenon is provided in works like [34, 35, 24, 39]. Based on these insights, this section proposes a method designed to train a substantial number of parameters, while selectively updating only a portion of the parameters at any one time to conserve computational resources.

Low-Rank Adaptation (LoRA) Introduced in [15], LoRA is designed specifically for the fine-tuning stage of model training.

Consider a pre-trained model with a weight matrix $\mathbf{W} \in \mathbb{R}^{m \times n}$ from a specific linear layer. LoRA proposes an innovative modification: transforming \mathbf{W} into $\mathbf{W} + \mathbf{BA}$. Here, $\mathbf{B} \in \mathbb{R}^{m \times r}$ and

$\mathbf{A} \in \mathbb{R}^{r \times n}$ are newly introduced matrices, where r is significantly smaller than both m and n . Then during fine-tuning, \mathbf{W} is kept frozen while matrices \mathbf{B} and \mathbf{A} are trained. At the inference stage, \mathbf{BA} is added to \mathbf{W} which preserves the model’s original structure. The matrix \mathbf{A} is initialized using Kaiming initialization [12], while \mathbf{B} is initially set to a zero matrix to ensure consistency.

SwiLoRA training process Now, let us delve deeper into the linear system $(\mathbf{W} + \mathbf{BA})\mathbf{x} = \mathbf{y}$. As illustrated in Figure 1, we decompose the matrix \mathbf{B} into its column vectors $\mathbf{b}_k \in \mathbb{R}^{m \times 1}$ for $k = 1, \dots, r$, represented as $\mathbf{B} = [\mathbf{b}_1, \dots, \mathbf{b}_r]$. Similarly, we decompose matrix \mathbf{A} into its row vectors $\mathbf{a}_k^T \in \mathbb{R}^{n \times 1}$ for $k = 1, \dots, r$, leading to $\mathbf{A}^T = [\mathbf{a}_1^T, \dots, \mathbf{a}_r^T]$. Hereafter, we call these vectors \mathbf{b}_k and \mathbf{a}_k as LoRA vectors.

The product \mathbf{BA} can be expressed using these LoRA vectors as follows:

$$\mathbf{BA} = \sum_{k=1}^r \mathbf{b}_k \mathbf{a}_k^T. \quad (1)$$

Let $\mathcal{C}(\mathbf{B})$ denote an ordered set containing $\min(m, n)$ vectors, each having the same dimensions as \mathbf{b}_k . Furthermore, ensure that $\{\mathbf{b}_1, \dots, \mathbf{b}_r\} \subset \mathcal{C}(\mathbf{B})$. Similarly, define $\mathcal{C}(\mathbf{A}^T)$ as an ordered set containing $\min(m, n)$ vectors, each having the same dimensions as \mathbf{a}_i . Also, let $\{\mathbf{a}_1^T, \dots, \mathbf{a}_r^T\} \subset \mathcal{C}(\mathbf{A}^T)$. Moving forward, we will refer to $\mathcal{C}(\mathbf{B})$ and $\mathcal{C}(\mathbf{A}^T)$ as the candidate vectors for \mathbf{B} and \mathbf{A} , respectively.

It is known for k matrices $\mathbf{W}_1, \mathbf{W}_2, \dots, \mathbf{W}_k$, there holds

$$\text{rank}\left(\sum_{i=1}^k \mathbf{W}_i\right) \leq \sum_{i=1}^k \text{rank}(\mathbf{W}_i). \quad (2)$$

If we adopt the strategy in LoRA to add \mathbf{BA} to \mathbf{W} and only update \mathbf{B} and \mathbf{A} from the pre-training stage, according to (2), the rank of updated parameters of the local linear system through the entire training process will be limited to $2r$. This limitation can potentially impede the training efficacy. To mitigate this issue, we alter the values of \mathbf{b}_k and \mathbf{a}_k to $\mathbf{b}'_k \in \mathcal{C}(\mathbf{B})$ and $\mathbf{a}'_k \in \mathcal{C}(\mathbf{A}^T)$ at appropriate frequencies, respectively, with these new values randomly selected from predefined candidate vectors list $\mathcal{C}(\mathbf{B})$ and $\mathcal{C}(\mathbf{A}^T)$ (one of \mathbf{b}'_k or \mathbf{a}'_k can be the same as \mathbf{b}_k or \mathbf{a}_k). To maintain the consistency of the model’s output, compensatory adjustments are made to \mathbf{W} . To be more precise, when \mathbf{b}_k and \mathbf{a}_k are updated to \mathbf{b}'_k and \mathbf{a}'_k , we accordingly adjust \mathbf{W} with the equation $\mathbf{W} \leftarrow \mathbf{W} + \mathbf{b}_k \mathbf{a}_k^T - \mathbf{b}'_k \mathbf{a}'_k^T$.

When implementing these updates, the updated parameters of both \mathbf{B} and \mathbf{A} are derived from $\min(m, n)$ distinct candidate vectors, which ensures updated parameters are full-rank. Readers can refer to [24, 41] for more details.

As previously mentioned, the model initially possesses full rank, and the rank of each layer decreases progressively over time. Consequently, we have adopted an exponential decay function for the switching frequency, where the coefficients are determined empirically. The selection of LoRA rank r for \mathbf{BA} is influenced by the final rank of the layers post-training, which has been extensively explored in LoRA and its variants [32, 37].

Currently Large Language Models (LLMs) predominantly utilize Adam [18] and AdamW [25] optimizers over SGD, which rely on optimizer states. It is crucial to note that after switching LoRA vectors, the gradients associated with these parameters are also changed, which prevents the reuse of optimizer states. To address this issue, when \mathbf{a}_k is switched, we reset the optimizer states of \mathbf{b}_k . And conversely, when \mathbf{b}_k is switched, we reset optimizer states of \mathbf{a}_k . Note that we reset optimizer states of counterpart pair rather than optimizer states of the switched parameters itself. This approach will be further explained in Section 3. Additionally, when the optimizer states are reset to zero, we freeze corresponding parameters for N steps to maintain the robustness of the training. In this study, N is set to 5.

The above process is described in Algorithm 1 and Algorithm 2.

Initialization of SwiLoRA Results in [11, 36] have demonstrated the importance of initialization of LoRA matrices \mathbf{B} and \mathbf{A} to the training effects. Unlike these works, which are applied only during the fine-tuning stage, our method is utilized throughout the entire training process. Moreover, zero initialization for $\mathcal{C}(\mathbf{B})$ encounters similar issues when switching candidates. Hence, we cannot

Algorithm 1 Switch algorithm: $\mathbf{W}, \mathbf{P}, \mathbf{Q} = \text{switch}(\mathbf{W}, \mathbf{P}, \mathbf{Q}, i, j)$. $\mathcal{C}(\mathbf{P})[i]$ is i -th predefined candidate vectors for \mathbf{P} .

Require: $\mathbf{W}, \mathbf{P}, \mathbf{Q}, i, j$

- 1: $\mathbf{W} \leftarrow \mathbf{W} + \mathbf{P}_{:,i} \mathbf{Q}_{i,:}$
 - 2: $\mathbf{P}_{:,i}, \mathcal{C}(\mathbf{P})[j] \leftarrow \mathcal{C}(\mathbf{P})[j], \mathbf{P}_{:,i}$
 - 3: $\text{opt_state}(\mathbf{Q}_{i,:}) \leftarrow \mathbf{0}$
 - 4: $\mathbf{W} \leftarrow \mathbf{W} - \mathbf{P}_{:,i} \mathbf{Q}_{i,:}$
 - 5: **return** $\mathbf{W}, \mathbf{P}, \mathbf{Q}$
-

Algorithm 2 SwiLoRA training process. $\text{switch_num}(step, r, interval_0, \theta)$ is an integer generator function which yields $\lfloor s \rfloor + X$ numbers sampled from 1 to r where $s = r / (interval_0 e^{\theta \cdot step})$ and random variable $X \sim \text{Bernoulli}(s - \lfloor s \rfloor)$, i.e. $P(X = 1) = 1 - P(X = 0) = s - \lfloor s \rfloor$.

Require: $interval_0, \theta, N$

- 1: **for** step **in** all training steps **do**
 - 2: Train model with Adam/AdamW optimizer for one step
 - 3: **for** all linear layers **do**
 - 4: **for** i in $\text{switch_num}(step, r, interval_0, \theta)$ **do**
 - 5: Sample $j \sim \{k\}_{k=1}^{\min(m,n)}$
 - 6: $\mathbf{W}, \mathbf{B}, \mathbf{A} \leftarrow \text{switch}(\mathbf{W}, \mathbf{B}, \mathbf{A}, i, j)$
 - 7: Freeze $\mathbf{A}_{i,:}$ for N steps
 - 8: **end for**
 - 9: **for** i in $\text{switch_num}(step, r, interval_0, \theta)$ **do**
 - 10: Sample $j \sim \{k\}_{k=1}^{\min(m,n)}$
 - 11: $\mathbf{W}^T, \mathbf{A}^T, \mathbf{B}^T \leftarrow \text{switch}(\mathbf{W}^T, \mathbf{A}^T, \mathbf{B}^T, i, j)$
 - 12: Freeze $\mathbf{B}_{:,i}$ for N steps
 - 13: **end for**
 - 14: **end for**
 - 15: **end for**
-

simply use the same initialization strategy for \mathbf{B} and \mathbf{A} as employed in LoRA. To achieve appropriate initialization for matrices \mathbf{B} and \mathbf{A} along with their candidate vectors, we follow the idea of Xavier initialization [8] and Kaiming initialization [12].

The main idea of [8] and [12] is to maintain a balance in the variance of the activations and gradients across layers during forward and backward propagation. In this study, we focus on balancing the variance of activations. Furthermore, we aim to ensure the updated parameters derived from \mathbf{B} are of the same amount as those derived from \mathbf{A} :

$$\Delta \mathbf{B} \mathbf{A} = \mathbf{B} \Delta \mathbf{A}. \quad (3)$$

In this paper, we fix the scaling factor of $\mathbf{B} \mathbf{A}$ to $\frac{1}{r}$. Then the weight matrix of the linear layer is modified to $\mathbf{W} + \frac{1}{r} \mathbf{B} \mathbf{A}$. To meet the above conditions, the standard deviation of initialization for \mathbf{B} and \mathbf{A} and their LoRA vectors are

$$\begin{aligned} \text{std}[\mathbf{B}] = \text{std}[\mathbf{b}] &= \left(\frac{r}{\sqrt{mn}}\right)^{\frac{1}{4}} \text{gain}^{\frac{1}{2}} \quad \forall \mathbf{b} \in \mathcal{C}(\mathbf{B}), \\ \text{std}[\mathbf{A}] = \text{std}[\mathbf{a}] &= \left(\frac{\sqrt{mr}}{\sqrt{nn}}\right)^{\frac{1}{4}} \text{gain}^{\frac{1}{2}} \quad \forall \mathbf{a} \in \mathcal{C}(\mathbf{A}^T), \end{aligned} \quad (4)$$

where gain is a constant dependent on the type of activation function used.

A detailed analysis of the above results is postponed to Section 3.

3 Theoretical analysis

In this section, we conduct a thorough discussion of our algorithm and address four key aspects:

1. Demonstrating that the order of LoRA vectors does not impact performance;

2. The effectiveness of our algorithm;
3. Discussion on resetting optimizer states;
4. Detailed process to deduce the values for initialization.

First, we take a closer look at the properties of the local linear system. Assume that the loss function of the model is denoted by \mathcal{L} . Our discussion focuses on the scenario where the input \mathbf{x} and output \mathbf{y} are vectors, satisfying the equation:

$$\mathbf{y} = (\mathbf{W} + \frac{1}{r}\mathbf{B}\mathbf{A})\mathbf{x}. \quad (5)$$

Next, we calculate the gradients of the column vectors of \mathbf{B} . Recall the decomposition of $\mathbf{B}\mathbf{A}$ as defined in the previous equations. For $k = 1, \dots, r$, the gradient of \mathbf{b}_k with respect to the loss function \mathcal{L} is given by:

$$\nabla_{\mathbf{b}_k}\mathcal{L} = (\mathbf{a}_k^T\mathbf{x})\nabla_{\mathbf{y}}\mathcal{L}. \quad (6)$$

Note that when the input \mathbf{x} is a vector, $\mathbf{a}_k^T\mathbf{x}$ becomes a scalar. Consequently, the gradients of \mathbf{b}_k are proportional to the gradients of \mathbf{y} .

We can also derive the gradients of the row vectors of \mathbf{A} as follows:

$$\nabla_{\mathbf{a}_k}\mathcal{L} = ((\nabla_{\mathbf{y}}\mathcal{L})^T\mathbf{b}_k)\mathbf{x}. \quad (7)$$

In this expression, $(\nabla_{\mathbf{y}}\mathcal{L})^T\mathbf{b}_k$ is a scalar, indicating that the gradients of \mathbf{a}_k are aligned in the direction of the input activations.

Independence of vectors updating In our algorithm, we randomly select candidate vectors to replace vectors in \mathbf{A} and \mathbf{B} , which alters the matching pairs of \mathbf{b}_k and \mathbf{a}_k . A natural question arises: Does the matching order of these vector pairs influence the training effects?

In the following discussion, we will use the notation $\tilde{\mathbf{v}}$ to denote trainable parameters that are initialized with the value of \mathbf{v} .

For the sake of clarity, we focus on one linear layer without a bias term for our discussion. We denote $\mathcal{L}(\tilde{\mathbf{W}}\mathbf{x})$ as the loss when the weight matrix of the linear layer under study is $\tilde{\mathbf{W}}$, with the vector \mathbf{x} as input activations. This formulation intentionally omits contributions from other layers and the bias term, as they are beyond the scope of our subsequent analysis.

To integrate the LoRA matrices while preserving the initial loss value, we reformulate $\mathcal{L}(\tilde{\mathbf{W}}\mathbf{x})$ as $\mathcal{L}((\mathbf{W} - \sum_k \mathbf{b}_k\mathbf{a}_k^T + \sum_k \tilde{\mathbf{b}}_k\tilde{\mathbf{a}}_k^T)\mathbf{x})$. Further, we simplify this expression to $\mathcal{L}(\mathbf{a}_1, \dots, \mathbf{a}_r; \mathbf{b}_1, \dots, \mathbf{b}_k; \mathbf{x})$. A simple observation is

$$\mathcal{L}(\mathbf{a}_1, \dots, \mathbf{a}_r; \mathbf{b}_1, \dots, \mathbf{b}_k; \mathbf{x}) = \mathcal{L}(\mathbf{0}, \dots, \mathbf{0}; \mathbf{0}, \dots, \mathbf{0}; \mathbf{x}). \quad (8)$$

Recall that the gradient $\nabla_{\mathbf{b}_k}\mathcal{L} = (\mathbf{a}_k^T\mathbf{x})\nabla_{\mathbf{y}}\mathcal{L}$. We derive the following expression:

$$\Delta\mathbf{b}_k\mathbf{a}_k^T = (c(\mathbf{a}_k^T\mathbf{x})\nabla_{\mathbf{y}}\mathcal{L} + \text{opt_state}(\mathbf{b}_k))\mathbf{a}_k^T, \quad (9)$$

where c is a negative value from optimizer and $\text{opt_state}(\mathbf{b}_k)$ is optimizer state of \mathbf{b}_k , determined by the value of $(\mathbf{a}_k^T\mathbf{x})\nabla_{\mathbf{y}}\mathcal{L}$ of previous steps. Moreover, the value of $\nabla_{\mathbf{y}}\mathcal{L}$ will remain unchanged, as indicated by (8). Consequently, the component $\Delta\mathbf{b}_k\mathbf{a}_k^T$ is influenced solely by \mathbf{a}_k and not by other LoRA vectors. Similarly, the value of $\mathbf{b}_k\Delta\mathbf{a}_k^T$ is influenced only by \mathbf{b}_k when switching \mathbf{a}_k . Note that the updated weight can be expressed as

$$(\mathbf{b}_k + \Delta\mathbf{b}_k)(\mathbf{a}_k^T + \Delta\mathbf{a}_k^T) - \mathbf{b}_k\mathbf{a}_k^T = \Delta\mathbf{b}_k\mathbf{a}_k^T + \mathbf{b}_k\Delta\mathbf{a}_k^T + \Delta\mathbf{b}_k\Delta\mathbf{a}_k^T, \quad (10)$$

where $\Delta\mathbf{b}_k\Delta\mathbf{a}_k^T$ represents a minor term that can generally be disregarded. Hence, the updates derived by \mathbf{b}_k and \mathbf{a}_k are independent.

From this discussion, we can conclude that the order of vectors \mathbf{a}_k and \mathbf{b}_k does not influence the parameter updates in the current step. For instance, for $1 \leq i, j \leq r$, back propagation of $\mathcal{L}(\mathbf{a}_1, \dots, \mathbf{a}_j, \dots, \mathbf{a}_i, \dots, \mathbf{a}_r; \mathbf{b}_1, \dots, \mathbf{b}_k; \mathbf{x})$ and $\mathcal{L}(\mathbf{a}_1, \dots, \mathbf{a}_i, \dots, \mathbf{a}_j, \dots, \mathbf{a}_r; \mathbf{b}_1, \dots, \mathbf{b}_k; \mathbf{x})$ yield the same parameters updating to the weight matrix of the linear layer.

Effectiveness of SwiLoRA Consider the following modification to the original model. For the weight matrix $\mathbf{W} \in \mathbb{R}^{m \times n}$ of a specific linear layer in the model, replace \mathbf{W} with the product of matrices $\mathbf{B}^0 \mathbf{A}^0$, where $\mathbf{B}^0 \in \mathbb{R}^{m \times \min(m,n)}$ and $\mathbf{A}^0 \in \mathbb{R}^{\min(m,n) \times n}$. This modification results in a full-rank weight matrix $\mathbf{B}^0 \mathbf{A}^0$ and introduces more parameters than the original model. Consequently, it is anticipated to achieve results that are at least as good as those of the original model when the full parameters of this modified model are trained.

We now compare the modified model with another model that implements the SwiLoRA strategy. Define $\mathbf{B}_{:,i}^0 = \mathcal{C}(\mathbf{B})[i]$ and $\mathbf{A}_{i,:}^0 = \mathcal{C}(\mathbf{A}^T)[i]^T$ for $i = 1, \dots, \min(m, n)$. It becomes apparent that the two models are quite the same except that the model applying SwiLoRA strategy updates only subsets of parameters incrementally.

In optimization, it is well-established that for problems with separable objective functions, the parameters of each separable group can be optimized independently. Although the loss function of the SwiLoRA model is not separable, the preceding discussion has demonstrated the independence between the LoRA vectors. Consequently, we can infer that the inseparable components of the loss function concerning parameters within the same linear layer are modest. Therefore, this suggests that training subsets of parameters incrementally, as in the SwiLoRA model, is likely more effective than other methods, such as the layer-wise training approach proposed in [2].

Reset of optimizer states Let us discuss whether it is reasonable to zero out the optimizer states of LoRA vectors and temporarily freezing them when switching their counterpart LoRA vectors.

Consider a scenario where \mathbf{b}_k is switched while \mathbf{a}_k is not. Note that, according to (8), the forward propagation remains unaffected after the switching occurs. During the initial step after switching \mathbf{b}_k , with \mathbf{a}_k being frozen, the only term contributing to the weight matrix update is $\Delta \mathbf{b}_k \mathbf{a}_k^T$ according to (10). We previously established that this term, $\Delta \mathbf{b}_k \mathbf{a}_k^T$ in (9), is not influenced by other LoRA vectors apart from \mathbf{a}_k . Consequently, changes made to \mathbf{b}_k or any other recently switched LoRA vectors do not impact the accuracy of the optimizer states for \mathbf{b}_k . This substantiates the rationale behind resetting the optimizer states.

If we choose not to freeze \mathbf{a}_k , we derive the following from a similar equation to (9):

$$\mathbf{b}_k \Delta \mathbf{a}_k^T = c((\nabla_{\mathbf{y}} \mathcal{L})^T \mathbf{b}_k) \mathbf{x} + \mathbf{b}_k \text{opt_state}(\mathbf{a}_k). \quad (11)$$

This formula demonstrates that without resetting \mathbf{a}_k , the update direction would be completely incorrect.

The reasoning for switching \mathbf{a}_k and its implications can be deduced in a similar manner.

Derivation of initialization Parameters We have provided the initial values of \mathbf{B} and \mathbf{A} in Section 2. Below, we present the deduction process.

The initial values of \mathbf{B} and \mathbf{A} were specified in Section 2. In this section, we present the derivation process.

As demonstrated in [12], consider two matrices, \mathbf{W}_1 and \mathbf{W}_2 , both characterized by zero mean and uniform distribution. The standard deviation (std) of the elements of their product is given by:

$$\text{std}[\mathbf{W}_1 \mathbf{W}_2] = \sqrt{k} \text{std}[\mathbf{W}_1] \text{std}[\mathbf{W}_2], \quad (12)$$

where k represents the output dimension of the matrix \mathbf{W}_1 . To ensure the stability of forward propagation, it is crucial that the output of each layer maintains a standard deviation of 1. However, when the matrix \mathbf{W}_2 represents activation values, its standard deviation, denoted as $\text{std}[\mathbf{W}_2] = \text{gain}$, differs from 1 due to the influence of the activation function. For ReLU activations, $\text{gain} = \sqrt{2}$. Following this principle, we derive:

$$\text{std}\left[\frac{1}{r} \mathbf{B} \mathbf{A} \mathbf{x}\right] = \frac{\sqrt{r}}{r} \text{std}[\mathbf{B}] \text{std}[\mathbf{A}] \sqrt{n} = \text{gain}. \quad (13)$$

The standard deviation of the gradients for LoRA vectors is given by:

$$\begin{aligned} \text{std}[\nabla_{\mathbf{b}_k} \mathcal{L}] &= \sqrt{n} \text{std}[\mathbf{a}_k] \text{std}[\mathbf{x}] \text{std}[\nabla_{\mathbf{y}} \mathcal{L}], \\ \text{std}[\nabla_{\mathbf{a}_k} \mathcal{L}] &= \sqrt{m} \text{std}[\mathbf{b}_k] \text{std}[\mathbf{x}] \text{std}[\nabla_{\mathbf{y}} \mathcal{L}]. \end{aligned} \quad (14)$$

Assuming the updated parameters are solely influenced by the gradients of the current step, to obtain $\frac{1}{r}\Delta BA \sim \frac{1}{r}B\Delta A$, the following condition must be met:

$$std[\nabla_{\mathbf{B}}\mathcal{L}\mathbf{A}] = std[\mathbf{B}\nabla_{\mathbf{A}}\mathcal{L}]. \quad (15)$$

From this, we derive:

$$\begin{aligned} std[\nabla_{\mathbf{B}}\mathcal{L}\mathbf{A}] &= \sqrt{r}std[\nabla_{\mathbf{b}_k}\mathcal{L}]std[\mathbf{A}], \\ std[\mathbf{B}\nabla_{\mathbf{A}}\mathcal{L}] &= \sqrt{r}std[\mathbf{B}]std[\nabla_{\mathbf{a}_k}\mathcal{L}]. \end{aligned} \quad (16)$$

By combining (13)-(16), we achieve the following standard deviations:

$$std(\mathbf{A}) = \left(\frac{\sqrt{mr}}{n\sqrt{n}}\right)^{\frac{1}{4}}gain^{\frac{1}{2}}, \quad std(\mathbf{B}) = \left(\frac{r}{\sqrt{mn}}\right)^{\frac{1}{4}}gain^{\frac{1}{2}}. \quad (17)$$

4 Experiments

4.1 Experimental setup

We designed our experiments based on the settings described in [24] to benefit from established hyperparameter configurations. Our studies are carried out on the LLaMA model [31], with model sizes reduced to 130M, 250M, and 350M. The specific hyperparameters for these models are detailed in Table 1. We use Adam optimizer to train the model with $\beta_1 = 0.9$, $\beta_2 = 0.999$. We use a cosine learning rate schedule with 100 warm-up steps and a total of 40,000 training steps. We employ the Adam optimizer for training, with $\beta_1 = 0.9$ and $\beta_2 = 0.999$. The experiments utilize the C4 dataset [6], with the first 46M samples of the training dataset serving as our training data, and samples from the entire validation dataset used for testing. The evaluation of validation loss is performed on 10M tokens for all our experiments, with evaluations conducted every 1,000 steps. All experiments are conducted using 8xNVIDIA Tesla A100 80GB PCIe GPUs. Gradient accumulation is applied when GPU memory reaches its limit.

Table 1: Model sizes and architectures used in our experiments

Params	Hidden	Heads	Layers	Batch size	Batch size per GPU	Seq. len.
130M	768	12	12	600	300	256
250M	768	16	24	1152	72	512
350M	1024	16	24	1152	72	512

In our experiments involving LoRA and SwiLoRA, we set the LoRA rank to 128 or 256. This rank is chosen based on previous findings [38, 24, 39] suggesting it is an effective approximation for models smaller than 1B. To ensure fairness across all experiments, the initialization method described in Section 2 is applied to both LoRA and SwiLoRA experiments. We deploy LoRA adapters across all attention layers and fully connected layers in these experiments.

For the hyperparameters in Algorithm 2, we initiate with $interval_0 = 40$ and set $N = 5$. The parameter θ is adjusted to ensure that the switching frequency is one-third of its initial frequency at the 1/10 of total steps.

All experiments were repeated multiple times to select the best results. The learning rates were selected from a predefined set, including 0.0002, 0.0005, 0.001, 0.002, 0.005, 0.01, ... The final chosen learning rates are detailed in Table 2.

Table 2: Learning rate settings for our experiments

	130M	250M	350M
Full-rank	0.001	0.001	0.001
LoRA(rank= 128)	0.01	0.01	0.01
SwiLoRA(rank= 128)	0.02	0.02	0.02
SwiLoRA(rank= 256)	\	0.02	0.02

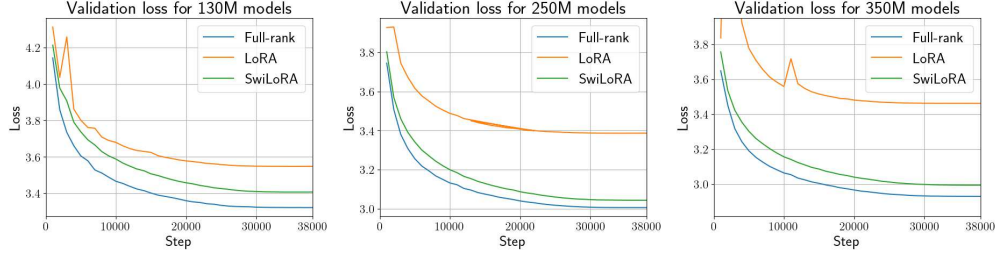


Figure 2: Loss results for 130M, 250M, and 350M models with a LoRA rank of 128.

4.2 Experimental results

Figure 2 displays the experimental results for the 130M, 250M, and 350M models, respectively, with the LoRA rank set to 128. The data reveal that while LoRA alone does not yield satisfactory training results, SwiLoRA approaches the performance of full-rank training. The performance gap continues to grow as model size increases. This suggests that the low-rank training approach, such as LoRA, might cause models to become trapped in local minima, while SwiLoRA mitigates this issue by dynamically changing trainable parameters.

Table 3: Perplexity results at step 38,000 for 130M, 250M, and 350M models.

	130M	250M	350M
Full-rank	27.71	20.19	18.72
LoRA(rank= 128)	34.74	29.56	31.87
SwiLoRA(rank= 128)	30.26	20.97	19.96
SwiLoRA(rank= 256)	\	19.82	18.70

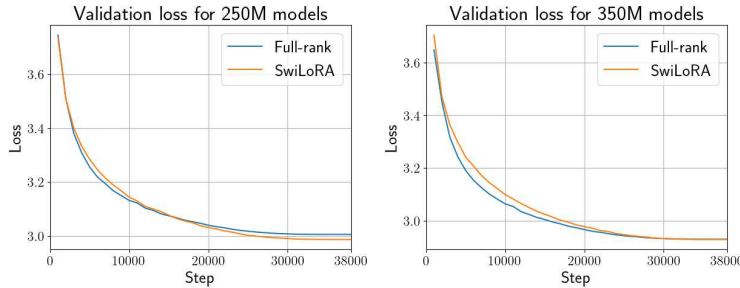


Figure 3: Loss results for 250M, and 350M models with a LoRA rank of 256.

As shown in Figure 3, additional experiments conducted on the 250M and 350M models with a LoRA rank of 256 demonstrates improved performance compared to those with the rank set at 128, achieving outcomes close to those of full-rank training. Although utilizing a higher rank yields better outcomes, we argue that it is more economical to increase the model size for larger models for several reasons. Firstly, the method still has potential for further refinement. Secondly, a lower LoRA rank enables training on devices with limited memory capacities. Furthermore, in the context of 3D parallelism, inter-node communication is predominantly influenced by data parallelism, where communication overhead are proportional to trainable parameters. The trainable parameters for each model are detailed in Table 4. For further discussions on potential ways to enhance the SwiLoRA strategy, refer to Section 5. And the impact of distributed training is detailed in Appendix F.

In our experiments, we observed that switching frequencies that are either too large or too small, as well as the specific shape of the switching frequency curve, negatively affect training accuracy. The freezing steps constant N also impacts the training accuracy. However, selecting an optimal value for N is relatively straightforward, as this value is robust across different model since it simply determines how many steps are needed to warm up switched LoRA vectors. Detailed investigations into the effects of these hyperparameters can be found in Appendix C.

Table 4: Comparison of trainable parameters: full-rank models vs. LoRA and SwiLoRA.

	130M	250M/128 rank	350M/128 rank	250M/256 rank	350M/256 rank
Full-rank	134.3M	247.5M	368.2M	247.5M	368.2M
(Swi)LoRA	71.7M	98.9M	125.6M	148.4M	185.4M

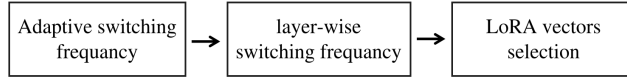


Figure 4: Future work roadmap.

5 Limitations and future work

We hypothesize that the LoRA ranks specified in [24] are sufficient for training to achieve the same loss as full-rank training when the trainable parameters are frequently changed. However, experiments have demonstrated that the accuracy does not match that of full-rank training if the LoRA rank is not large enough. Besides, tuning the switching frequency of the LoRA vectors’ curve is challenging. To address these limitations, we propose the following directions for future work, as illustrated in Figure 4.

- In our experiments, we simply used exponentially decreasing switching frequencies, which may not be the optimal approach. Conducting extensive experiments to determine the best frequencies across all steps is nearly impossible. Therefore, guidelines should be developed to help set appropriate switching frequencies throughout the training process.
- Going further, a more detailed idea is to examine each layer of the model to adjust the switching frequencies. For instance, LoRA-drop [40] evaluates whether the rank is sufficient using a norm of $\Delta \mathbf{W}\mathbf{x}$. This is rational because different types of layers, such as the Q, K, V matrices in transformer layers, exhibit significantly varied behaviors. Similarly, shallow and deep layers respond differently.
- In our work, we simply chose candidate vectors at random. However, during training, all candidates are updated separately, leading to significant difference among them. The selection of these candidates may influence the training outcomes. Thanks to the relatively long switching interval(exceeding 40 steps in our experiments), it is feasible to perform some time-consuming operations to determine the weights of the candidates for selection.

6 Conclusions

In this work, we introduce SwiLoRA, a novel training strategy designed for parameter-efficient pre-training. Our approach achieves comparable accuracy to full-rank training while reducing the trainable parameters to approximately 50% to 60% of those in traditional full-rank training throughout the entire process. Moreover, the computational overhead and memory usage are nearly identical to those of LoRA when using the same number of trainable parameters. Additionally, we provide a theoretical analysis of our algorithm to confirm its correctness and to offer insights into its training methodology. The empirical results and theoretical analysis support our perspective on training: One can keep model parameters unchanged while change the part of trainable parameters during the training dynamically to achieve efficacy similar to full training.

References

- [1] Dan Alistarh, Torsten Hoefer, Mikael Johansson, Nikola Konstantinov, Sarit Khirirat, and Cédric Renggli. The convergence of sparsified gradient methods. In Samy Bengio, Hanna M. Wallach, Hugo Larochelle, Kristen Grauman, Nicolò Cesa-Bianchi, and Roman Garnett, editors, *Advances in Neural Information Processing Systems 31: Annual Conference on Neural Information Processing Systems 2018, NeurIPS 2018, December 3-8, 2018, Montréal, Canada*, pages 5977–5987, 2018.
- [2] Yoshua Bengio, Pascal Lamblin, Dan Popovici, and Hugo Larochelle. Greedy layer-wise training of deep networks. In Bernhard Schölkopf, John C. Platt, and Thomas Hofmann, editors, *Advances in Neural Information Processing Systems 19, Proceedings of the Twentieth Annual Conference on Neural Information Processing Systems, Vancouver, British Columbia, Canada, December 4-7, 2006*, pages 153–160. MIT Press, 2006.
- [3] Davis W. Blalock, Jose Javier Gonzalez Ortiz, Jonathan Frankle, and John V. Guttag. What is the state of neural network pruning? In Inderjit S. Dhillon, Dimitris S. Papailiopoulos, and Vivienne Sze, editors, *Proceedings of Machine Learning and Systems 2020, MLSys 2020, Austin, TX, USA, March 2-4, 2020*. mlsys.org, 2020.
- [4] Jeffrey Dean, Greg Corrado, Rajat Monga, Kai Chen, Matthieu Devin, Mark Mao, Marc' aurelio Ranzato, Andrew Senior, Paul Tucker, Ke Yang, Quoc Le, and Andrew Ng. Large scale distributed deep networks. In F. Pereira, C.J. Burges, L. Bottou, and K.Q. Weinberger, editors, *Advances in Neural Information Processing Systems*, volume 25. Curran Associates, Inc., 2012.
- [5] Tim Dettmers, Artidoro Pagnoni, Ari Holtzman, and Luke Zettlemoyer. Qlora: Efficient finetuning of quantized llms, 2023.
- [6] Jesse Dodge, Maarten Sap, Ana Marasović, William Agnew, Gabriel Ilharco, Dirk Groeneveld, Margaret Mitchell, and Matt Gardner. Documenting large webtext corpora: A case study on the colossal clean crawled corpus, 2021.
- [7] Jonathan Frankle and Michael Carbin. The lottery ticket hypothesis: Finding sparse, trainable neural networks. In *International Conference on Learning Representations*, 2019.
- [8] Xavier Glorot and Yoshua Bengio. Understanding the difficulty of training deep feedforward neural networks. In *Proceedings of the thirteenth international conference on artificial intelligence and statistics*, pages 249–256. JMLR Workshop and Conference Proceedings, 2010.
- [9] Suriya Gunasekar, Blake E. Woodworth, Srinadh Bhojanapalli, Behnam Neyshabur, and Nati Srebro. Implicit regularization in matrix factorization. In Isabelle Guyon, Ulrike von Luxburg, Samy Bengio, Hanna M. Wallach, Rob Fergus, S. V. N. Vishwanathan, and Roman Garnett, editors, *Advances in Neural Information Processing Systems 30: Annual Conference on Neural Information Processing Systems 2017, December 4-9, 2017, Long Beach, CA, USA*, pages 6151–6159, 2017.
- [10] Song Han, Jeff Pool, John Tran, and William J. Dally. Learning both weights and connections for efficient neural networks. *CoRR*, abs/1506.02626, 2015.
- [11] Soufiane Hayou, Nikhil Ghosh, and Bin Yu. Lora+: Efficient low rank adaptation of large models, 2024.
- [12] Kaiming He, Xiangyu Zhang, Shaoqing Ren, and Jian Sun. Delving deep into rectifiers: Surpassing human-level performance on imagenet classification, 2015.
- [13] Shwai He, Liang Ding, Daize Dong, Miao Zhang, and Dacheng Tao. Sparseadapter: An easy approach for improving the parameter-efficiency of adapters, 2022.
- [14] Neil Houlsby, Andrei Giurgiu, Stanislaw Jastrzebski, Bruna Morrone, Quentin de Laroussilhe, Andrea Gesmundo, Mona Attariyan, and Sylvain Gelly. Parameter-efficient transfer learning for nlp, 2019.
- [15] Edward J Hu, yelong shen, Phillip Wallis, Zeyuan Allen-Zhu, Yuanzhi Li, Shean Wang, Lu Wang, and Weizhu Chen. LoRA: Low-rank adaptation of large language models. In *International Conference on Learning Representations*, 2022.
- [16] Yanping Huang, Youlong Cheng, Ankur Bapna, Orhan Firat, Dehao Chen, Mia Xu Chen, Hyoungho Lee, Jiquan Ngiam, Quoc V. Le, Yonghui Wu, and Zhifeng Chen. Gpipe: Efficient training of giant neural networks using pipeline parallelism. In Hanna M. Wallach, Hugo Larochelle, Alina Beygelzimer, Florence d'Alché-Buc, Emily B. Fox, and Roman Garnett, editors, *Advances in Neural Information Processing Systems 32: Annual Conference on Neural Information Processing Systems 2019, NeurIPS 2019, December 8-14, 2019, Vancouver, BC, Canada*, pages 103–112, 2019.
- [17] Hyesung Jeon, Yulhwa Kim, and Jae-Joon Kim. L4Q: parameter efficient quantization-aware training on large language models via lora-wise LSQ. *CoRR*, abs/2402.04902, 2024.
- [18] Diederik P. Kingma and Jimmy Ba. Adam: A method for stochastic optimization, 2014.

- [19] Mu Li, David G. Andersen, Jun Woo Park, Alexander J. Smola, Amr Ahmed, Vanja Josifovski, James Long, Eugene J. Shekita, and Bor-Yiing Su. Scaling distributed machine learning with the parameter server. In Jason Flinn and Hank Levy, editors, *11th USENIX Symposium on Operating Systems Design and Implementation, OSDI '14, Broomfield, CO, USA, October 6-8, 2014*, pages 583–598. USENIX Association, 2014.
- [20] Xiang Lisa Li and Percy Liang. Prefix-tuning: Optimizing continuous prompts for generation, 2021.
- [21] Yixiao Li, Yifan Yu, Chen Liang, Pengcheng He, Nikos Karampatziakis, Weizhu Chen, and Tuo Zhao. Loftq: Lora-fine-tuning-aware quantization for large language models. *CoRR*, abs/2310.08659, 2023.
- [22] Zhiyuan Li, Yuping Luo, and Kaifeng Lyu. Towards resolving the implicit bias of gradient descent for matrix factorization: Greedy low-rank learning. In *International Conference on Learning Representations*, 2021.
- [23] Zhuohan Li, Eric Wallace, Sheng Shen, Kevin Lin, Kurt Keutzer, Dan Klein, and Joseph E. Gonzalez. Train large, then compress: Rethinking model size for efficient training and inference of transformers. *CoRR*, abs/2002.11794, 2020.
- [24] Vladislav Lialin, Sherin Muckatira, Namrata Shivagunde, and Anna Rumshisky. ReLoRA: High-rank training through low-rank updates. In *Workshop on Advancing Neural Network Training: Computational Efficiency, Scalability, and Resource Optimization (WANT@NeurIPS 2023)*, 2023.
- [25] Ilya Loshchilov and Frank Hutter. Decoupled weight decay regularization. In *7th International Conference on Learning Representations, ICLR 2019, New Orleans, LA, USA, May 6-9, 2019*. OpenReview.net, 2019.
- [26] Deepak Narayanan, Mohammad Shoeybi, Jared Casper, Patrick LeGresley, Mostofa Patwary, Vijay Anand Korthikanti, Dmitri Vainbrand, Prethvi Kashinkunti, Julie Bernauer, Bryan Catanzaro, Amar Phanishayee, and Matei Zaharia. Efficient large-scale language model training on gpu clusters using megatron-lm, 2021.
- [27] Samyam Rajbhandari, Jeff Rasley, Olatunji Ruwase, and Yuxiong He. Zero: memory optimizations toward training trillion parameter models. In Christine Cuicchi, Irene Qualters, and William T. Kramer, editors, *Proceedings of the International Conference for High Performance Computing, Networking, Storage and Analysis, SC 2020, Virtual Event / Atlanta, Georgia, USA, November 9-19, 2020*, page 20. IEEE/ACM, 2020.
- [28] Mohammad Shoeybi, Mostofa Patwary, Raul Puri, Patrick LeGresley, Jared Casper, and Bryan Catanzaro. Megatron-lm: Training multi-billion parameter language models using model parallelism. *CoRR*, abs/1909.08053, 2019.
- [29] Sebastian U. Stich, Jean-Baptiste Cordonnier, and Martin Jaggi. Sparsified SGD with memory. In Samy Bengio, Hanna M. Wallach, Hugo Larochelle, Kristen Grauman, Nicolò Cesa-Bianchi, and Roman Garnett, editors, *Advances in Neural Information Processing Systems 31: Annual Conference on Neural Information Processing Systems 2018, NeurIPS 2018, December 3-8, 2018, Montréal, Canada*, pages 4452–4463, 2018.
- [30] Yang Sui, Miao Yin, Yu Gong, Jinqi Xiao, Huy Phan, and Bo Yuan. Elrt: Efficient low-rank training for compact convolutional neural networks, 2024.
- [31] Hugo Touvron, Thibaut Lavril, Gautier Izacard, Xavier Martinet, Marie-Anne Lachaux, Timothée Lacroix, Baptiste Rozière, Naman Goyal, Eric Hambro, Faisal Azhar, Aurelien Rodriguez, Armand Joulin, Edouard Grave, and Guillaume Lample. Llama: Open and efficient foundation language models, 2023.
- [32] Mojtaba Valipour, Mehdi Rezagholizadeh, Ivan Kobzyev, and Ali Ghodsi. DyLoRA: Parameter-efficient tuning of pre-trained models using dynamic search-free low-rank adaptation. In Andreas Vlachos and Isabelle Augenstein, editors, *Proceedings of the 17th Conference of the European Chapter of the Association for Computational Linguistics*, pages 3274–3287, Dubrovnik, Croatia, May 2023. Association for Computational Linguistics.
- [33] Ashish Vaswani, Noam Shazeer, Niki Parmar, Jakob Uszkoreit, Llion Jones, Aidan N Gomez, Łukasz Kaiser, and Illia Polosukhin. Attention is all you need. In I. Guyon, U. Von Luxburg, S. Bengio, H. Wallach, R. Fergus, S. Vishwanathan, and R. Garnett, editors, *Advances in Neural Information Processing Systems*, volume 30. Curran Associates, Inc., 2017.
- [34] Hongyi Wang, Saurabh Agarwal, and Dimitris Papailiopoulos. Pufferfish: Communication-efficient models at no extra cost, 2021.
- [35] Hongyi Wang, Saurabh Agarwal, Pongsakorn U-chupala, Yoshiki Tanaka, Eric Xing, and Dimitris Papailiopoulos. Cuttlefish: Low-rank model training without all the tuning. 2023.
- [36] Longteng Zhang, Lin Zhang, Shaohuai Shi, Xiaowen Chu, and Bo Li. Lora-fa: Memory-efficient low-rank adaptation for large language models fine-tuning. *CoRR*, abs/2308.03303, 2023.

- [37] Qingru Zhang, Minshuo Chen, Alexander Bukharin, Nikos Karampatziakis, Pengcheng He, Yu Cheng, Weizhu Chen, and Tuo Zhao. Adalora: Adaptive budget allocation for parameter-efficient fine-tuning, 2023.
- [38] Jiawei Zhao, Yifei Zhang, Beidi Chen, Florian Schäfer, and Anima Anandkumar. Inrank: Incremental low-rank learning, 2023.
- [39] Jiawei Zhao, Zhenyu Zhang, Beidi Chen, Zhangyang Wang, Anima Anandkumar, and Yuandong Tian. Galore: Memory-efficient LLM training by gradient low-rank projection. *CoRR*, abs/2403.03507, 2024.
- [40] Hongyun Zhou, Xiangyu Lu, Wang Xu, Conghui Zhu, and Tiejun Zhao. Lora-drop: Efficient lora parameter pruning based on output evaluation, 2024.
- [41] Bojia Zi, Xianbiao Qi, Lingzhi Wang, Jianan Wang, Kam-Fai Wong, and Lei Zhang. Delta-lora: Fine-tuning high-rank parameters with the delta of low-rank matrices. *CoRR*, abs/2309.02411, 2023.

A Related work

Similar to our approach, various LoRA variants employ strategies to increase the rank of a matrix by integrating weights into \mathbf{W} . For instance, ReLoRA [24] merges \mathbf{BA} into \mathbf{W} and then restarts training at regular intervals. However, resetting all LoRA adapter parameters can lead to unstable training. To address this, ReLoRA introduces random optimizer pruning and a jagged schedule, but it still requires 33% of the steps to be full-rank training. Delta-LoRA [41], another variant, focuses on the fine-tuning phase. It updates the matrix \mathbf{W} by using the gradients of the LoRA matrices \mathbf{B} and \mathbf{A} simultaneously as they are updated. It improve accuracy for fine-tuning. However, it appears to be insufficient in increasing the rank of the modified parameters.

An attractive feature of LoRA is its support for quantization without loss of accuracy. This is achieved by training the LoRA adapter matrices \mathbf{BA} with high precision, while keeping the frozen part \mathbf{W} at low precision within transformer layers. Examples of such quantization include QLoRA [5], LoftQ [21], and L4Q [17]. Additionally, the integration of quantization into SwiLoRA presents an intriguing topic. The feasibility of this integration is discussed in Appendix D.

On the other hand, LoRA and SwiLoRA are closely connected to SVD methods, although they do not require performing singular value decomposition. In fact, some studies utilize SVD to identify the most significant components of the decomposition of \mathbf{BA} . For instance, earlier work by Pufferfish [34] and subsequent work in Cuttlefish[35] introduce adaptive strategies to determine the necessary steps for full-rank training and to select the rank of each linear layer for low-rank decomposition. InRank [38] develops a low-rank training approach based on greedy low-rank learning [22]. Another recent study, GaLore [39], employs SVD to apply a low-rank structure for approximating gradients, offering greater memory efficiency compared to LoRA. While these works are promising on pre-training, they require the computation of SVD, which has a time complexity of $O(n^3)$ for $n \times n$ matrices. This computational demand becomes prohibitive for models with billions of parameters.

Table 5 provides a feature comparison among several related works discussed above.

Table 5: Comparison of different LoRA variations: LoRA, SwiLoRA, QLoRA and ReLoRA.

	SwiLoRA	LoRA	QLoRA	GaLore	ReLoRA
Few (trainable) parameters	✓	✓	✓✓	✓✓	✓
Fast computation	✓✓	✓✓	✓✓	✗	✓✓
Easy implementation	✓	✓✓	✗	✓	✓
Effective at pre-training	✓✓	✗	✓	✓✓	✓

B Implementation of LoRA vector switching

The primary distinction in the implementation of SwiLoRA from conventional approaches lies in its handling of gradients and optimizer states at the granularity of row or column vectors within matrix parameters. Consider the scenario when using the AdamW optimizer: typically, each trainable parameter group in AdamW is associated with a “step” state which is implemented as a float scalar value in the code. To facilitate the resetting of specific rows or columns in matrices, we modify the type of “step” in the optimizer to a 32-bit float matrix with the same shape as the corresponding parameters. In fact, this modification does incur some extra memory overhead. An alternative approach would be to implement “step” as a row vector for \mathbf{A} and a column vector for \mathbf{B} . However, this would require more complex code management, and thus, we have not adopted this strategy in our implementation.

With the capability to manipulate optimizer states and gradients at the level of rows and columns, we can now execute operations such as resetting optimizer states and freezing specific rows or columns of parameter matrices.

Additionally, note that all candidate vectors are stored in GPU memory, which consumes a modest amount of GPU resources. This portion of memory can be reduced by offloading the candidate vectors that are not actively in use to the CPU.

Table 6 presents a throughput comparison between SwiLoRA and LoRA under the same conditions described in Section 4, with the LoRA rank set to 128. The results demonstrate that the throughput of SwiLoRA is comparable to that of LoRA in single GPU experiments. Additionally, experiments conducted on an 8-GPU setup reveal a more pronounced difference between LoRA and SwiLoRA, which may be attributed to CPU overhead. There is potential for further reductions in overhead through code optimization. This is feasible since all operations involve lower order time complexity.

Table 6: The throughput of SwiLoRA and LoRA for the 350M model, with a total batch size of 1152 and varying batch sizes per GPU for gradient accumulation. All experiments were conducted on a single A100 GPU, except for the final one, which utilized 8 A100 PCIe GPUs.

	Batch sizes per GPU				Batch size on 8 GPUs
	1	18	36	72	72
LoRA	155s/step	16.5s/step	15.4s/step	14.8s/step	1.97s/step
SwiLoRA	159s/step	16.9s/step	15.9s/step	15.1s/step	2.37s/step

C Ablation study

In this section, we mainly use the 130M model with a LoRA rank of 128 and a batch size of 128. For hyperparameters not explicitly mentioned, we follow the configurations detailed in Section 4.

In Figure 5, we did two experiments. In the first experiment, we evaluate the model’s performance with varying descent rates for frequencies while maintaining a constant initial switching interval of 40. In the second experiment, we maintain a consistent descent rate for frequencies as detailed in Section 4, but we vary the initial switching interval across different experiments. It is evident from our results that both hyperparameters significantly impact training accuracy.

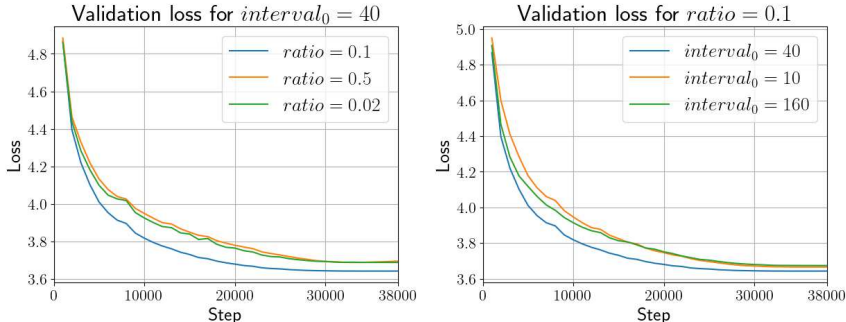


Figure 5: Loss comparison for the 130m model with different $interval_0$ and $ratio$, where the parameter $ratio$ determines the point at which the switching frequency is reduced to one-third of its initial value, occurring at the step $total_step \times ratio$.

In Figure 6, we conduct a series of experiments with various frequency settings. The results indicate that the choice of frequency settings plays a crucial role in the model’s effectiveness. Specifically, we find that setting both the initial frequency values and the descent rates to moderate levels is essential for achieving optimal performance. Extremely high or low frequency settings tend to degrade the model’s performance, indicating a sensitive balance that must be maintained.

In Figure 7, we conduct experiments to investigate the impact of the number of frozen steps N . The results show that the choice of N influences the loss outcomes. This can be explained as follows: when N is excessively large, the training parameters may become biased towards different subsets of the data. Conversely, if N is too small, at the moment the freezing is canceled, the gradients will have a larger contribution to the parameter updates due to the nature of momentum-based optimizers. This leads to potentially abrupt changes in model behavior.

In Figure 8, we present the results from a focused comparative study where we evaluated our initialization strategy against the traditional LoRA initialization method through two distinct experiments.

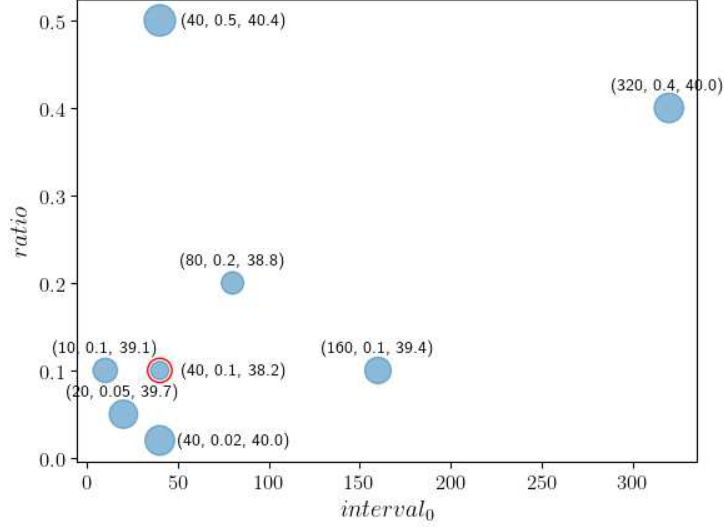


Figure 6: Perplexity comparison for the 130m model with different switching frequencies. The parameter $ratio$ determines the point at which the switching frequency is reduced to one-third of its initial value, occurring at the step $total_step \times ratio$.

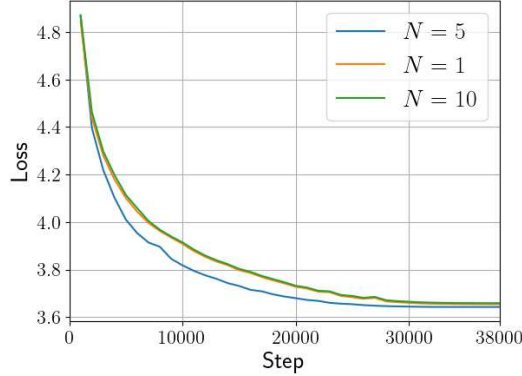


Figure 7: Comparison of loss for the 130m model at different values of N .

The results indicate that our initialization method outperform traditional approach for initialization. Notably, the loss curve for LoRA initialization reveals a slower decrease in initial loss compared to that of SwiLoRA initialization. This phenomenon in LoRA initialization can be attributed to the slow warm-up of matrix \mathbf{A} and its associated candidate vectors due to (7). In contrast, our method modifies the initialization values to allow for more rapid adjustments, enabling the model to adapt more effectively to the training data.

D Feasibility of quantization

Among all the LoRA variants that can be integrated into SwiLoRA, a quantization method such as QLoRA shows the most promise in enhancing efficiency and reducing memory usage. However, implementing quantization without significant accuracy loss is not straightforward. Given that LoRA vectors are frequently switched in SwiLoRA, the errors introduced by quantization can significantly impact the algorithm’s performance. For instance, when merging delta parameters triggered by the switching of LoRA vectors, the operation can be expressed as:

$$\mathbf{W} \leftarrow \text{quant}(\text{dequant}(\mathbf{W}) + \mathbf{b}_k \mathbf{a}_k^T - \mathbf{b}'_k \mathbf{a}'_k). \quad (18)$$

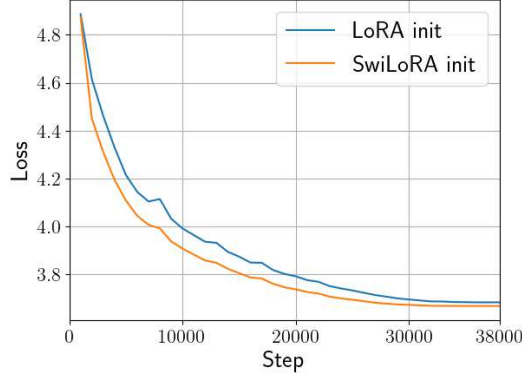


Figure 8: Loss comparison for the 130m model between traditional and our enhanced initialization methods.

Here, precision errors may arise, with values approximately equal to

$$\text{quant}(\mathbf{b}_k \mathbf{a}_k^T - \mathbf{b}'_k \mathbf{a}'_k{}^T) - (\mathbf{b}_k \mathbf{a}_k^T - \mathbf{b}'_k \mathbf{a}'_k{}^T). \quad (19)$$

Actually, it is possible to slightly adjust the values of candidate vectors before their selection to minimize this error. However, developing an efficient algorithm that effectively reduces this error without compromising accuracy is challenging. Therefore, we plan to explore this issue in future work.

E Distribution of Singular values

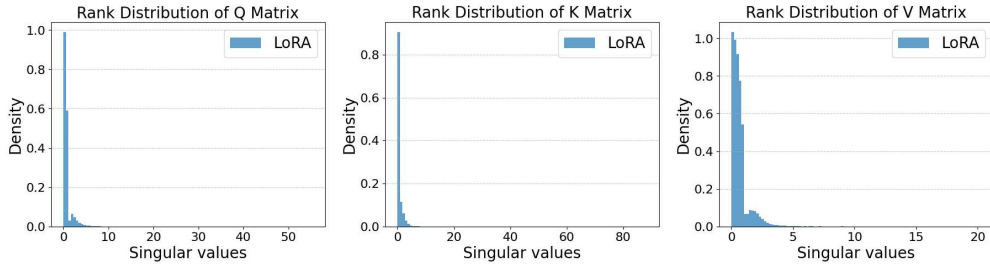


Figure 9: Rank distribution of LoRA on different types of linear layers.

Given that the rank distribution significantly influences the training efficacy of models [15, 7], we conducted experiments to examine the rank distribution of SwiLoRA. As outlined in Section 4, experiments were conducted on 350M model to analyze the rank distribution of linear layers after 40,000 training steps. Figure 9 demonstrates that the singular values of weight matrices converge within a limited range when trained with LoRA, indicating dominance of LoRA adapters in the linear layers. This dominance is expected, as the singular value distribution of weight matrices during the pre-training phase exhibits a form of illness, due to updates being limited to the low-rank adapter BA. In contrast, as illustrated in Figure 10, the rank distribution of SwiLoRA closely approximates that of full-rank training, suggesting a healthier and more effective adaptation process.

F Impact on distributed training

As demonstrated in [27], for a transformer model with n layers and a hidden dimension of h , the memory required for model parameters scales proportionally with nh^2 . Assuming these parameters are stored in $fp16/bf16$ format occupying Ψ parameters, the memory footprint for optimizer states would be approximately 12Ψ bytes when using the Adam optimizer as stated in [27]. Additionally, when the batch size is b and the sequence length is s , the memory consumption for activations scales

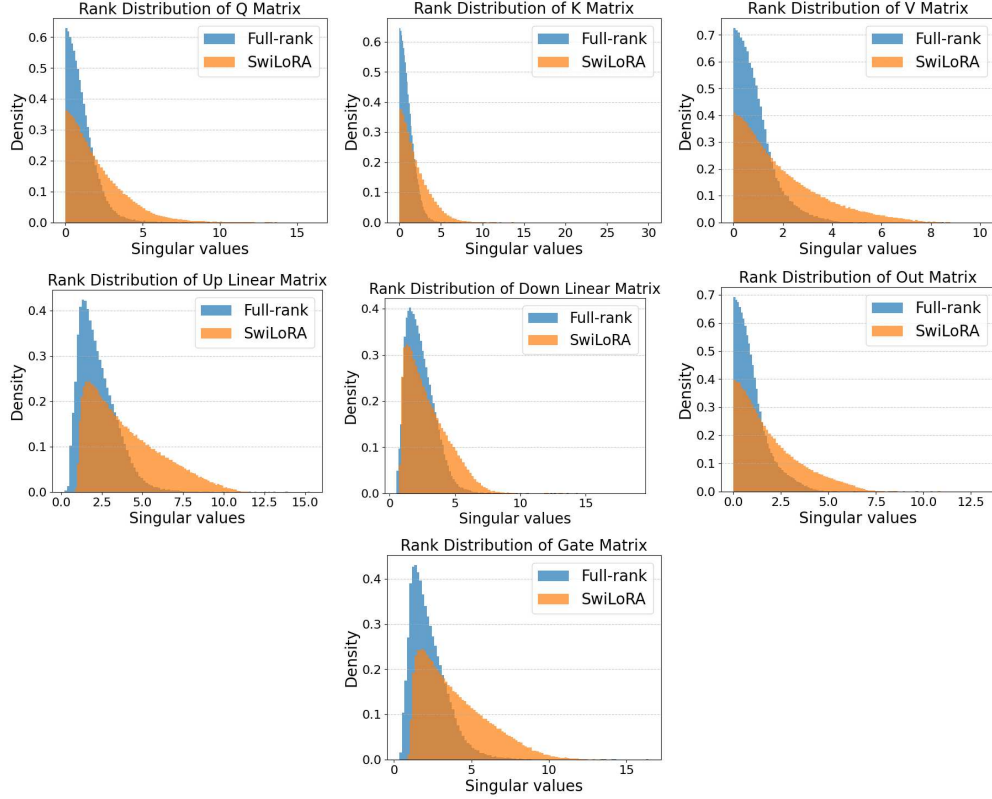


Figure 10: Rank distribution of full-rank training and SwiLoRA on different types of linear layers.

with *bshn*. To manage memory demands for large models, gradient accumulation can be utilized to adjust the batch size per GPU to 1. Moreover, activation checkpointing can be implemented to reduce memory consumption, though it comes with a trade-off: a 33% increase in computational overhead.

In this work, we primarily focus on the memory consumption associated with optimizer states, which constitutes a significant portion of the overall memory usage for models with tens of billions of parameters. Assuming that full-rank training requires knh^2 bytes of memory, where k is a constant. Our algorithm, as well as LoRA, reduces memory usage from knh^2 to $2knhr$, with r representing the LoRA rank.

In addition to memory usage, parameter-efficient training also reduces communication overhead. When implementing 3D parallelism to train large language models, tensor parallelism is typically limited within a single machine due to its substantial communication demands. Pipeline parallelism introduces some idle “bubble” time, which cannot be eliminated even with fast communication. And its communication overhead remains relatively low. The main part of inter-node communication stems from data parallelism, where the same amount of gradients as parameters is communicated at every training step. Consequently, having fewer trainable parameters can significantly decrease communication overhead. Moreover, reduced memory consumption allows a larger portion of the model to reside on a single GPU, potentially decreasing the degree of pipeline parallelism needed and consequently reducing the associated “bubble” time.